CALCULATION OF THE ABSORBED DOSE AND DOSE EQUIVALENT INDUCED BY MEDIUM-ENERGY NEUTRONS AND PROTONS AND COMPARISON WITH EXPERIMENT[1]

T. W. Armstrong and B. L. Bishop

Oak Ridge National Laboratory
Oak Ridge, Tennessee, 37830

Monte Carlo calculations have been carried out to determine the absorbed dose and dose equivalent for 592-MeV protons incident on a cylindrical phantom and for neutrons from 580-MeV proton-Be collisions incident on a semi-infinite phantom. For both configurations, the calculated depth dependence of the absorbed dose is in good agreement with experimental data.

INTRODUCTION

Nucleon-meson cascade calculations were recently carried out for monoenergetic neutrons (60 to 3000 MeV) and protons (400 to 3000 MeV) normally incident on a semi-infinite slab of tissue (ref. 1). For several incident energies, the calculated depth dependence of the absorbed dose was compared with available experimental results (ref. 2), which were obtained using somewhat different source-geometry configurations, and substantial differences were found. It was not clear from these comparisons whether the theory was in error or whether the differences could be ascribed to the different configurations used in the calculations and experiments.

The calculations have been carried out for two configurations: 592-MeV protons incident on a cylindrical phantom, and neutrons from 580-MeV proton-Be collisions incident on a semi-infinite slab phantom. The calculated depth distributions for the absorbed dose are compared with the measured distributions of Baarli and Goebel (ref. 2) for these same configurations. The depth distributions for the dose equivalent have also been calculated.

The method of calculation used is summarized in the next section, and the results are presented and discussed in the last section.

CALCULATIONAL METHOD

The method of calculation is the same as that described previously (ref. 1), so only a brief account of the calculational method will be given here. The calculations were carried out using the Monte Carlo code NMTC (ref. 3). This code takes into account charged-particle energy loss due to ionization and excitation of atomic electrons, elastic and nonelastic nucleon-nucleus and pion-nucleus collisions, pion and muon decay in flight and at rest, and negative-pion capture at rest. The electron-photon cascade resulting from the decay of neutral pions and the electrons and positrons from muon decay are included in an approximate manner (ref. 1). At energies above 15 MeV for nucleons and 2.2 MeV for charged pions, the energy, direction, and multiplicity of particles produced in nucleon-nucleus and pion-nucleus collisions are calculated using the intranuclear-cascade-evaporation model of nuclear reactions (refs. 4, 5). Proton-nucleus collisions below 15 MeV and pion-nucleus collisions below 2.2 MeV (except for the capture of negative pions at rest) are neglected. Neutron collisions below 15 MeV are treated using experimental cross-section data (ref. 3) in conjunction with the evaporation model (ref. 5) to determine particle production from neutron-nucleus nonelastic collisions. A detailed description of the method of calculation is given elsewhere (ref. 1).

The calculations have been carried out using tissue for the phantom composition. The following concentrations were used for the tissue (in at. %): H, 63.3; O, 25.8; C, 9.5; N, 1.4. A tissue density of 1.0 g/cm^3 was used.

RESULTS AND DISCUSSION

Incident Protons

The geometry for the case of 592-MeV incident protons is shown in figure 1. The protons are incident normally on one end of a cylindrical phantom

200 cm in depth by 50 cm in diameter. The experimental spatial variation of the incident proton intensity (ref. 2) was approximated in the calculations as a Gaussian distribution with a full-width-at-half-maximum value of 30 cm.

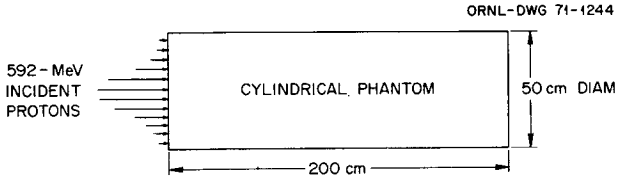

FIGURE 1.— Configuration for incident protons.

The depth dependence of the absorbed dose is shown in figure 2. The experimental absorbed dose is not given in absolute units, and thus only the shapes of the calculated and experimental distributions can be compared. Also shown for comparison in figure 2 is the absorbed dose calculated for a cylinder of infinite radius. This case corresponds to the configuration considered in the previous calculations (ref. 1), i.e., an infinitely broad beam incident on a semi-infinite slab. As shown in figure 2, the shape of the calculated distribution is in very good agreement with the experimental distribution when the cylindrical geometry used in experiment is simulated in the calculations. Therefore, for a meaningful comparison with the experimental absorbed-dose distribution it is necessary that the finite radius of the phantom be taken into account in the calculations.

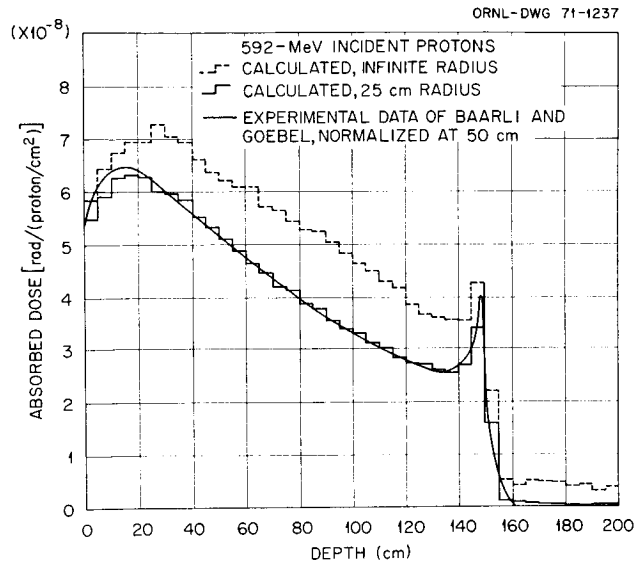

FIGURE 2.— Depth dependence of absorbed dose for 592-MeV incident protons.

The contributions to the absorbed dose and dose equivalent from various kinds of particles have also been calculated, and these are shown in figures 3 and 4 for the finite-radius geometry. The total dose is obtained by adding all of the contributions shown in the figures. The histogram labeled "primary ionization" in figure 3 gives the dose from the excitation and ionization of atomic electrons by those incident protons which have not undergone nuclear collision. The histogram labeled "secondary protons" gives the absorbed dose from the excitation and ionization of atomic electrons by protons produced from nonelastic nucleon-nucleus and pion-nucleus collisions and from the elastic collisions of nucleons and pions with hydrogen nuclei. The histogram labeled "heavy nuclei" gives the absorbed dose from particles with mass number greater than one produced from nonelastic nucleon-nucleus and pion-nucleus collisions and the absorbed dose from the recoiling nuclei produced from elastic neutron-nucleus collisions and from nonelastic nucleon-nucleus and pion-nucleus collisions. The histogram labeled "charged pions" gives the absorbed dose from the excitation and ionization of atomic electrons by both positively and negatively charged pions produced from nucleon-nucleus and pion-nucleus nonelastic collisions. The histogram labeled "photons from neutral pions" gives the absorbed dose from the electron-photon

cascade produced by the photons which arise from the decay of neutral pions. The histogram labeled "electrons, positrons, and photons" gives the absorbed dose from the electrons and positrons produced by muon decay and the absorbed dose from the photons produced by nucleon-nucleus and pion-nucleus nonelastic collisions. The histogram labeled "muons" gives the absorbed dose from the excitation and ionization of atomic electrons by both positively and negatively charged mu-mesons.

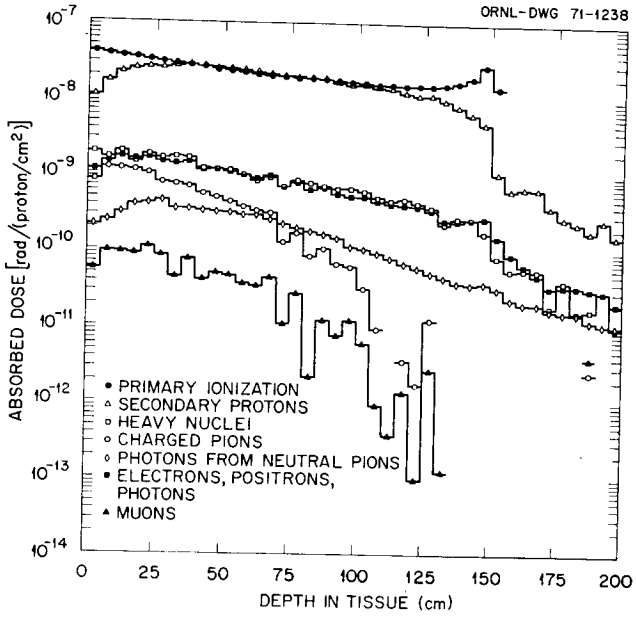

FIGURE 3.— Contribution of various particles to the absorbed dose for 592-MeV protons incident on a cylindrical phantom.

The histograms in figure 4 have meanings similar to those of figure 3 but correspond to the dose equivalent from various kinds of secondary particles. The calculation of the dose equivalent was carried out taking the quality factor to be a function of the linear energy transfer as in the previous calculations. In the case of protons, the damage curve given in reference 6, which is based on the recommendations of the National Committee on Radiation Protection and Measurements, was used. In the case of charged pions and muons, the quality factor as a function of linear energy transfer was taken to be the same as that for protons, and damage curves for charged pions and muons, constructed in a manner similar to the proton damage curve given in reference 6, were used. A quality factor of 20 was assigned to the energy deposited by all heavy nuclei and a quality factor of unity was assigned to the energy deposited by electrons, positrons, and photons.

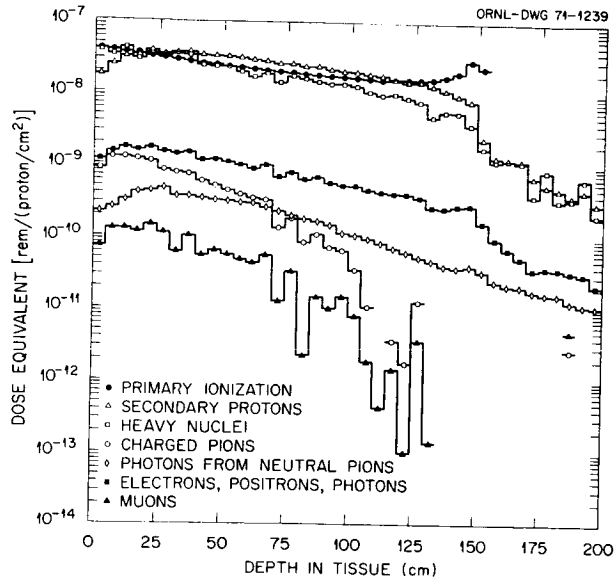

FIGURE 4.— Contribution of various particles to the dose equivalent for 592-MeV protons incident on a cylindrical phantom.

The contributions to the absorbed dose and dose equivalent by various kinds of particles have also been calculated for the case of a cylinder with infinite radius, and these results are given in reference 7.

Incident Neutrons

The experimental arrangement used by Baarli and Goebel (ref. 2) to measure the absorbed dose from incident neutrons is shown schematically in figure 5. The neutrons produced from proton-Be interactions at angles of 18° and 56° with respect to the proton beam were directed toward an absorber of tissue-like material, and the depth dependence of the absorbed dose was measured. The neutron intensity on the absorber was approximately uniform over a circular area 15 cm in radius. The energy spectrum of the incident neutrons was not measured. A "nominal" energy for the neutron beam was calculated by Baarli and Goebel assuming only elastic collisions in the target. These nominal energies are 525 MeV and 180 MeV for scattering angles of 18° and 56°, respectively (ref. 2). In the previous calculations for the depth dependence of the absorbed dose (ref. 1), all of the incident neutrons were assumed to be monoenergetic at energies of 525 or 180 MeV.

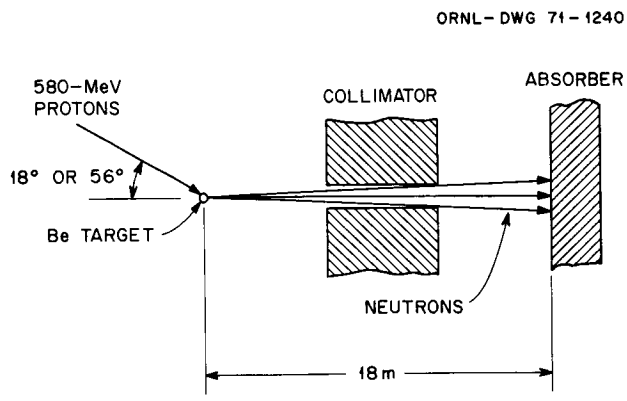

FIGURE 5.— Configuration for incident neutrons.

To obtain an estimate of the incident neutron spectrum, the energy distribution of neutrons from 580-MeV protons incident on Be was calculated using the intranuclear-cascade model (ref. 4). The results, in terms of the differential neutron production cross section, are shown in figure 6. In calculating the neutron production spectrum, the production averaged over the angular intervals from 15.5° to 20.5° and from 51° to 61° were used to represent the production at 18° and 56°, respectively. It is evident from figure 6 that representing these spectra by monoenergetic neutrons at 180 MeV and 525 MeV, as was done in the previous calculations (ref. 1), is a gross oversimplification.

The depth dependence of the absorbed dose for the case of incident neutrons is shown in figures 7 and 8. The histograms labeled "180-MeV spectrum" and "525-MeV spectrum" were calculated using the incident neutron spectra shown in figure 6. The histograms labeled "180 MeV" and "525 MeV" are taken from the previous calculation (ref. 1) for monoenergetic incident neutrons. Since the experimental results are not reported in absolute units, they have been normalized to the present calculated results at a depth of 8 cm. The measured and calculated depth dependences of the absorbed dose are in good agreement when the energy distribution of the incident neutrons is taken into account in the calculations.

The results in figures 7 and 8 have been normalized on a per-incident-neutron basis. The results could have been normalized per proton-Be interaction. Letting N be the number of neutrons incident on the absorber per proton-Be interaction,

$$N = \frac{\Delta\Omega'}{\sigma_{inel}} \int_0^\infty dE \left(\frac{\Delta^2\sigma}{\Delta E \Delta\Omega} \right),$$

where $(\Delta^2\sigma/\Delta E\Delta\Omega)$ is given in figure 6, σ_{inel} is the Be inelastic cross section for protons at 580 MeV (= 210.7 mb, from the intranuclear-cascade calculations), and $\Delta\Omega'$ is the solid angle for neutrons from the target hitting the absorber, which can be obtained from the geometry of the experiment $[\Delta\Omega' = \pi(15)^2/(1800)^2]$. The values of N are 0.95×10^{-4} and 0.29×10^{-4} for the production angles of 18° and 56°, respectively.

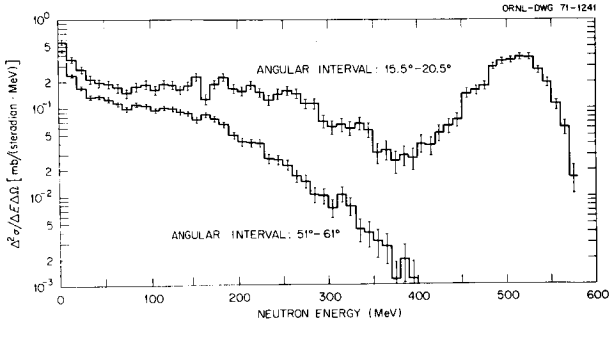

FIGURE 6.— Calculated differential neutron production cross section for 580-MeV protons incident on Be.

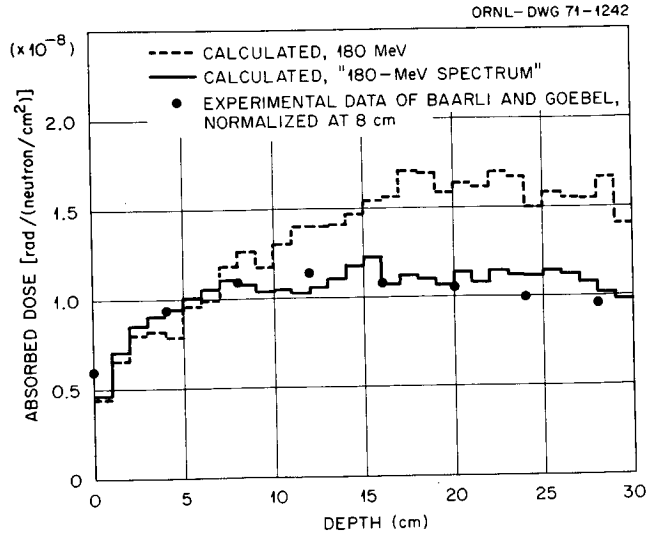

FIGURE 7.— Depth dependence of absorbed dose for neutrons incident on an infinite slab of tissue.

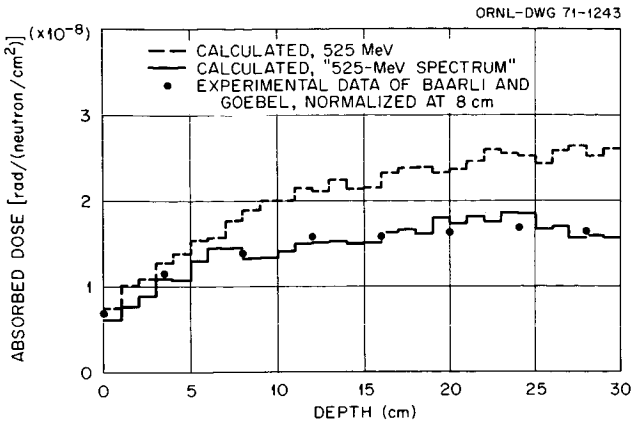

FIGURE 8.— Depth dependence of absorbed dose for neutrons incident on an infinite slab of tissue.

The contributions of various kinds of particles to the absorbed dose and the dose equivalent have also been calculated for the case of incident neutrons, and these results are given in reference 7.

In summary, the good agreement between the present calculations and the measurements indicates that the disagreement between the previous calculations (ref. 1) and measurements was a result of not taking into account some of the details of the experiment in the calculations and not due to any shortcomings of the calculational method.

[1]This work was partially funded by the National Aeronautics and Space Administration, Order H-38280A, under Union Carbide Corporation's contract with the U. S. Atomic Energy Commission.

REFERENCES

1. ALSMILLER, R.G., Jr.; ARMSTRONG, T.W.; and COLEMAN, W.A.: Nucl. Sci. Eng. Vol. 42, 1970, p. 367.

2. BAARLI, J.; and GOEBEL, K.: Properties of High-Energy Beams from a 600-MeV Synchrocyclotron. Proc. XIth International Congress of Radiology, Rome, September 1965.

3. COLEMAN, W.A.; and ARMSTRONG, T.W.: The Nucleon-Meson Transport Code NMTC. Oak Ridge National Laboratory Document ORNL-46-6, 1970.

4. BERTINI, H.W.: Phys. Rev. Vol. 188, 1969, p. 1711.

5. GUTHRIE, Miriam P.: EVAP-4: Another Modification of a Code to Calculate Particle Evaporation from Excited Compound Nuclei. Oak Ridge National Laboratory Document ORNL-TM-3119, 1970.

6. TURNER, J.E. et al., Health Physc. vol. 10, 1964, p. 783

7. ARMSTRONG, T.W.; and BISHOP, B.L.: Calculation of the Absorbed Dose and Dose Equivalent Induced by Medium-Energy Neutrons and Protons and Comparison with Experiment. Oak Ridge National Laboratory Document ORNL-TM-3304 (in press).